Sensors and Materials, Vol. 37, No. 12 (2025) 5373–5384
MYU Tokyo

S & M 4250

A Portable Electronic Nose for Real-time Monitoring of Food Spoilage Using Multiple Machine Learning Models

Pikulkaew Tangtisanon* and Boonyawee Grodniyomchai

Department of IoT and Information Engineering, School of Engineering,
King Mongkut's Institute of Technology Ladkrabang, Bangkok 10520, Thailand

(Received August 29, 2025; accepted October 2, 2025)

Keywords: electronic nose, odor classification, machine learning, portable device, gas sensor

In this study, we present the design and development of a portable electronic nose (E-nose) system for detecting and classifying spoiled household food through the application of machine learning (ML) techniques. The targeted odors include fungi from bread, spoiled rice, spoiled milk, yoghurt, rotten egg, rotten boiled egg, rotten pork, and rotten beef, totaling eight odor classes. A total of 1800 samples were collected using three gas sensors and one temperature sensor. After outlier removal with Isolation Forest, 1000 samples remained. Multiple ML models were trained and evaluated over ten iterations, comparing classification accuracy and processing time. Among all the models, the k-nearest neighbor (KNN) achieved the highest performance, with an average accuracy of 99.889% and an average processing time of 0.167477 s. The decision tree (DT) model followed closely with an accuracy of 99.843% and required a significantly less processing time of 0.012080 s. Although DT has a slightly lower accuracy than KNN, its processing time is 13.86 times faster. For our scenario that requires real-time results, DT is a better choice than KNN. The proposed portable E-nose demonstrates strong potential for real-world applications such as food spoilage detection, environmental monitoring, and health diagnostics.

1. Introduction

Odor detection and classification play a vital role in various real-world applications such as food safety, environmental monitoring, health diagnostics, and hazardous chemical detection. Traditionally, odor assessment has relied on the human odor perception system, which is inconsistent and vulnerable since the sensitivity of human perception can decrease over time because of external factors. The development of electronic noses (E-noses) has become an effective technological solution that addresses this problem. The devices use arrays of chemical sensors that detect airborne substances and convert them into digital signals, simulating the human sense of smell. E-nose systems are capable of accurately and efficiently classifying these signals into different odor categories by using machine learning (ML) algorithms.

*Corresponding author: e-mail: pikulkaew.ta@kmitl.ac.th
https://doi.org/10.18494/SAM5894

ISSN 0914-4935
https://myukk.org/

E-noses have been developed and used in various fields such as disease diagnosis,[1] food quality control,[2,3] and environmental assessment, utilizing sensors such as MOSs and metal-organic frameworks to detect gases. Prior research has demonstrated their effectiveness in tasks such as evaluating Baijiu Jiuqu fermentation quality,[3] identifying whey protein contamination in milk powder[4] and black tea with superior quality,[5] and diagnosing diabetes from exhaled breath using ethanol and acetone sensors.[6] Furthermore, E-noses have proven useful in industrial textile fragrance essences[7] and in detecting toxic airborne chemicals such as benzene and toluene with portable sensing devices.[8] To enhance odor detection and classification accuracy, researchers have employed various ML techniques such as principal component analysis,[4] support vector machines (SVMs),[9,10] artificial neural networks,[10,11] artificial immune systems,[12] long short-term memory–convolutional neural network (LSTM–CNN),[7] and ensemble learning methods.[13,14] These approaches allow for more robust signal processing and classification performance, enabling broad adoption across industries. Jiang *et al.*[7] developed a portable E-nose featuring a MEMS-based SnO_2 MOS gas sensor array with 18 sensor variants doped with Pd, Pt, and Ru at various loadings, optimized through a genetic algorithm for the detection and classification of four industrial fragrance essences typically utilized in textile manufacturing. These essences primarily contain aromatic alcohols and esters, many of which include overlapping compounds such as linalool, benzyl acetate, and D-limonene, creating considerable classification difficulties. Employing a combined LSTM–CNN deep learning model, the device reached classification accuracies of 96.9% for single essences and 94.2% for complex mixtures, outperforming human olfactory abilities.

In this study, we designed a prototype portable E-nose based on the methodology from Lu *et al.*,[15] which requires a gas chamber, various types of gas sensor, and a fan to draw odors in and out. This device was developed to assist elderly individuals, people with olfactory impairments, and those with visual impairments in avoiding the consumption of spoiled food, thereby promoting better health and safety. To achieve this goal, we conducted experiments to classify common spoiled foods frequently consumed in daily life, such as spoiled milk, rotten egg, and rotten beef. Compared with previous portable E-nose designs,[6,16] our system achieves a balance between using fewer sensors and maintaining a high classification accuracy, while also reducing the processing time. Machine learning models were used with datasets collected from the proposed E-nose, and various models were trained and tested with training and testing datasets to find the most efficient model. The results of each model were analyzed to determine the most suitable candidate for real-time odor prediction in the portable E-nose, aiming to achieve a balance between classification accuracy and processing time.

2. Materials and Methods

In this section, we will focus on the design of a portable E-nose, which must include gas sensors capable of detecting various gases, an E-nose with a gas chamber, and fans for drawing in and expelling odors. It will also cover samples of food odors commonly encountered in daily life and the evaluation of ML models to predict odors. All models were implemented using standard configurations, where all parameters were set to default values in scikit-learn. K-nearest

neighbors (KNNs) were configured with n_neighbors = 8. For SVM, the probability parameter was enabled and a linear kernel was employed. The decision tree (DT) was initialized with random_state = 0. The neural network (NN) was configured with hidden_layer_sizes = (512, 256, 64), activation = relu, solver = lbfgs, learning_rate_init = 0.0001, max_iter = 1000, and tol = 0.000001. Linear regression (Linear R) and logistic regression (Logistic R) models were used with their default settings. All training and testing procedures were executed on an HP Omen 15-AX201TX laptop equipped with an Intel Core i7-7700HQ CPU, Nvidia GeForce GTX 1050 GPU, 16 GB of DDR4 RAM (2400 MHz), and a 1 TB WD Black SN770 SSD, and running Windows 10 (64-bit).

2.1 Gas sensor

E-nose systems can be equipped with a variety of commercial gas sensors, which are divided into three groups according to their modes of operation: conductivity, gravimetric, and optical sensors. Because of its exceptional sensitivity to a wide variety of gases, such as volatile organic compounds (VOCs), alcohols, ammonia, and hydrogen, MOS sensors, a form of conductivity sensor, are frequently utilized in gas detection systems. When gas molecules encounter the heated metal oxide surface, these sensors detect changes in electrical resistance. The quick reaction and recovery time of MOS sensors is one of its main benefits, making them appropriate for real-time monitoring applications. Additionally, they have a rather simple design and are cheap to manufacture, making them perfect for small and affordable devices. Furthermore, MOS sensors are famous for their robustness and extended operational life in stable environments. Despite being occasionally viewed as a drawback, their wide cross-sensitivity can be advantageous when employed in sensor arrays to identify complex gas patterns. Because of these features, MOS sensors are frequently used in industrial safety applications, environmental research, and portable air quality monitoring. These factors led us to decide to build our E-nose system using MOS sensors.

2.2 E-nose

The portable E-nose device consists of a gas chamber, two fans (one for absorbing odor into the chamber and one for exhausting odor from the chamber, the strengths of which can be adjusted), three gas sensors (MQ-2, MQ-7, and MQ-135), and a temperature sensor. These sensors are commercial products manufactured by Winsen Electronics Co., Ltd. Data are transmitted via an RS-485 port with the Modbus RTU protocol, which is widely used in industrial plants, as shown in Fig. 1.

The proposed E-nose device is equipped with two fans positioned on the left and right sides of the chamber. Prior to the experiment, the right fan was activated to ventilate the chamber for 30 min. Data were recorded at 1 s intervals throughout this process. Once the sensor readings stabilized, the target odor sample was placed in front of the left fan. Then, the left fan was turned on and the right fan was turned off to allow the odor to enter the chamber. Sensor data were collected until 1800 samples were obtained. After collecting the required data, the left fan was

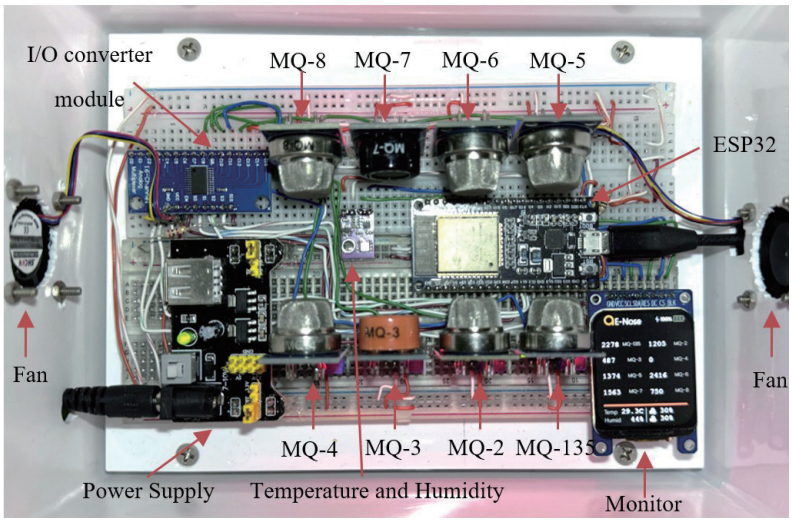

Fig. 1. (Color online) Electronic nose chamber.

turned off and the right fan was turned on again to expel the odor from the chamber until the sensor readings return to their baseline values.

2.3 Dataset

The odor datasets from the E-nose used in this research are of eight types, namely, fungi from bread, spoiled rice, spoiled milk, yoghurt, rotten egg, rotten boiled egg, rotten pork, and rotten beef. The features of the dataset were collected by the sensors in the E-nose, consisting of MQ-2, MQ-7, and MQ-135 gas sensors, along with a temperature sensor. The MQ sensors output analog-to-digital converter (ADC) values, which represent gas concentration levels. Temperature is measured in degrees Celsius (°C). The details of the sensors are shown in Table 1 and an example of the odor dataset is shown in Table 2.

The MQ-2, MQ-7, and MQ-135 gas sensors, along with a temperature sensor, were selected owing to their relatively similar response patterns to a variety of odor-related compounds. This characteristic enables a more consistent sensing profile across devices and makes these sensors suitable candidates for future implementation in compact and portable detection systems.

The data obtained from the sensors were collected at a rate of one sample per second for 30 min, resulting in 1800 samples. The outliers in the dataset were removed using Isolation Forest (iForest), which is an anomaly detection algorithm proposed by Liu *et al.*[18] It identifies anomalies on the basis of the concept of data isolation, removing outliers from 1800 to 1000 samples of each odor. The formulas used for iForest are shown in Eqs. (1)–(3). Then, the dataset was split into two subsets: a training set consisting of 70% and a testing set consisting of 30% of the total number of samples. After that, the samples were fed through multiple models to assess and compare their performance characteristics as shown in Fig. 2. The samples were fed into each model in ten separate runs, and the accuracy and processing time were obtained by

Table 1
Gas sensors.[17]

Sensor	Detection	Detection range (ppm)
MQ-2	Flammable gas (propane, butane), smoke	300–10000
MQ-7	Carbon monoxide	10–500
MQ-135	Air pollution (ammonia, sulfide, benzene, smoke, carbon dioxide)	10–1000

Table 2
Example of the odor dataset.

Odor	Label	MQ-2 (ADC)	MQ-7 (ADC)	MQ-135 (ADC)	Temp (°C)
Fungi	0	495	1035	653	43.2
Spoiled rice	1	2502	1281	423	45.4
Spoiled milk	2	1021	1072	771	41.2
Yoghurt	3	487	1011	270	41.9
Rotten egg	4	468	951	582	43.6
Rotten boiled egg	5	467	970	592	43.6
Rotten pork	6	713	1071	778	42.2
Rotten beef	7	2309	1501	492	44.9

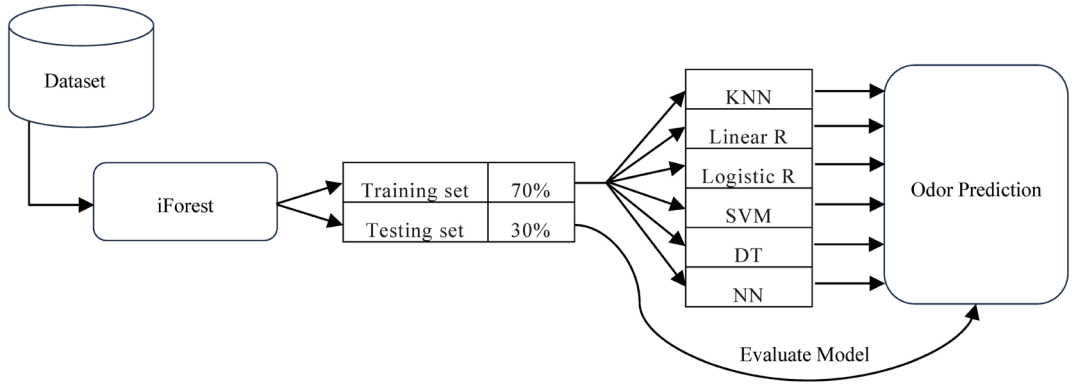

Fig. 2. Machine learning model training and testing schematic.

averaging the results. The following ML models were used in this research: KNN, Linear R, Logistic R, SVM, DT, and NN.

$$c(n) = 2H(n-1) - \left(\frac{2(n-1)}{n}\right) \tag{1}$$

$$H(i) = \sum_{k=1}^{i} \frac{1}{k} \tag{2}$$

$$s(x,n) = 2^{-\frac{E(h(x))}{c(n)}} \tag{3}$$

Here, $h(x)$ is the path length of instance x and $c(n)$ is the average path length across all isolation trees.

2.4 Evaluation

The evaluation of the research used the confusion matrix and accuracy to compare the performance of the ML models, measured as a percentage. The formulas used for the confusion matrix are shown in Eqs. (4)–(9), and that for the standard deviation (*SD*) is shown in Eq. (10).

$$Accuracy = \frac{TP + TN}{TP + TN + FP + FN} \tag{4}$$

$$Precision = \frac{TP}{TP + FP} \tag{5}$$

$$Recall = \frac{TP}{TP + FN} \tag{6}$$

$$Specifity = \frac{TN}{TN + FP} \tag{7}$$

$$F1\text{-}score = \frac{2 \cdot Precision \cdot Recall}{Precision + Recall} \tag{8}$$

$$Confusion\,Matrix = \begin{bmatrix} TP & FP \\ FN & TN \end{bmatrix} \tag{9}$$

Here, *TP* is true positive, *TN* is true negative, *FP* is false positive, and *FN* is false negative.

$$SD = \sqrt{\frac{\sum_i \left(x_i - \bar{x}\right)^2}{\left(n-1\right)}} \tag{10}$$

Here, $\bar{x}$ is the mean of the sample group, x_i is the value of the i sample in the group, and n is the number of samples in the group

3. Experimental Results

Table 3 shows the average classification accuracy as a percentage for six models: KNN, Linear R, Logistic R, SVM, DT, and NN. The models were evaluated across a total of ten trials. The results showed that KNN, DT, and SVM displayed consistent performance, with mean

Table 3
Comparison of average classification accuracy (%) across different ML models.

#	KNN	Linear R	Logistic R	SVM	DT	NN
1	99.83	12.03	94.12	99.50	99.96	99.54
2	99.83	12.47	93.42	99.75	99.92	99.79
3	99.88	11.24	93.25	99.42	99.88	99.50
4	99.92	11.88	93.46	99.46	99.96	99.71
5	99.92	12.79	93.50	99.46	99.75	99.58
6	99.96	11.39	93.75	99.38	99.88	23.42
7	99.75	11.95	93.38	99.29	99.79	99.62
8	99.88	11.94	93.58	99.54	99.96	99.71
9	99.96	12.83	94.25	99.62	99.62	24.83
10	99.96	11.26	93.96	99.62	99.71	99.71
Mean	99.889	11.978	93.667	99.504	99.843	84.541
SD	0.069514	0.581928	0.338856	0.133683	0.119541	31.84389
Max	99.96	12.83	94.25	99.75	99.96	99.79
Min	99.75	11.24	93.25	99.29	99.62	23.42

accuracies of 99.889, 99.843, and 99.504%, respectively. Logistic R showed a mean accuracy of 93.667% with an *SD* of 0.33886, indicating that this model is less stable than KNN, DT, and SVM. NN performed less reliably with a lower accuracy of 84.541% and an *SD* of 31.8439, which is the highest *SD* among all the models, indicating highly unstable and widely dispersed results. Linear R demonstrated the lowest performance, with a mean accuracy of only 11.98% and an *SD* of 0.58193. The best performance across trials was shown by KNN, which had the highest average accuracy of 99.889% and the lowest *SD* of 0.06951.

Table 4 presents a comparison of the average processing times across all ten experimental trials for different ML models. Linear R achieved the fastest processing time overall but exhibited the lowest accuracy, making it unsuitable for practical use. DT ranked second (0.01208 s), followed by KNN (0.16748 s), SVM (0.44714 s), and NN (186.8075 s). DT demonstrated a significantly faster processing time, which is approximately 13.86 times faster than that of KNN. Although DT exhibits a slightly lower accuracy and a higher standard deviation than KNN, its significantly faster processing time makes it a strong candidate for applications that require immediate or real-time responses.

Sample data of rotten beef and spoiled milk odors obtained from the sensors are shown in Figs. 3 and 4, respectively. Each sample on the *X*-axis represents sensor data collected every second for 30 min. The *Y*-axis represents analog-to-digital converter (ADC) values acquired from the gas sensors using the ESP32 microcontroller. A total of 1800 samples were collected from the MQ-2, MQ-7, MQ-135, and temperature sensors, and subsequently reduced to 1000 samples after outlier removal using iForest.

Figure 3 shows the sensor responses of rotten beef. MQ-2 exhibited the highest signal amplitude at approximately 2000, whereas MQ-7 produced consistently high responses to approximately 1500. MQ-135 signals remained stable at approximately 500, and the temperature was maintained constant, ensuring consistent experimental conditions. Figure 4 shows the sensor responses of spoiled milk. MQ-7 exhibited the highest signal amplitude at approximately 1000, whereas MQ-2 produced responses around 900 with notable variation. MQ-135 signals

Table 4
Processing time comparison for odor classification models using E-nose data.

#	KNN	Linear R	Logistic R	SVM	DT	NN
1	0.167553	0.006981	0.198020	0.470758	0.012996	230.6476
2	0.209546	0.010230	0.204616	0.502965	0.010971	215.5576
3	0.159607	0.005985	0.179520	0.386047	0.012968	224.8997
4	0.179520	0.005984	0.192485	0.434810	0.011968	219.6047
5	0.166277	0.003990	0.186141	0.449797	0.013963	235.3572
6	0.161599	0.003989	0.226906	0.496674	0.011001	9.363463
7	0.146607	0.003989	0.149599	0.318168	0.013946	253.5403
8	0.160889	0.004985	0.202466	0.421883	0.010006	246.0792
9	0.167559	0.004985	0.261846	0.476332	0.010007	8.624973
10	0.155616	0.003988	0.193509	0.513973	0.012971	224.4004
Mean	0.167477	0.005510	0.199511	0.447141	0.012080	186.8075
SD	0.017103	0.001963	0.029492	0.060194	0.001508	94.4265
Max	0.209546	0.010230	0.261846	0.513973	0.013963	253.5403
Min	0.146607	0.003988	0.149599	0.318168	0.010006	8.624973

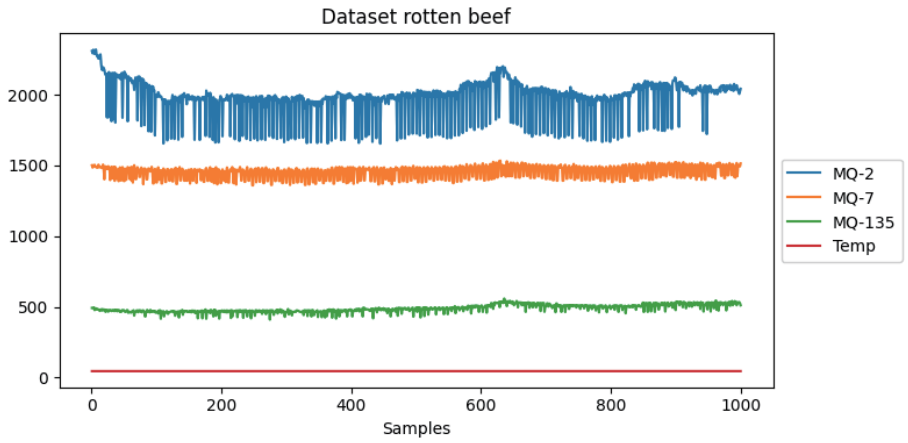

Fig. 3. (Color online) Sensor responses during rotten beef odor sampling.

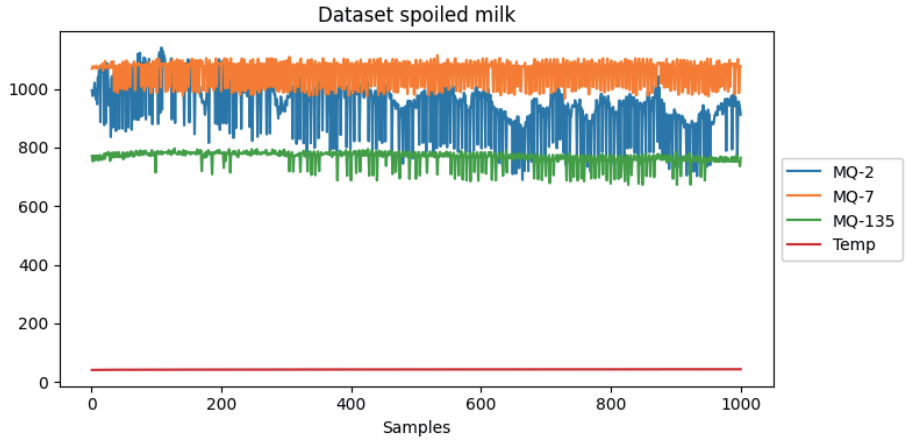

Fig. 4. (Color online) Sensor responses during spoiled milk odor sampling.

remained stable at approximately 750, and the temperature was maintained constant, ensuring consistent experimental conditions

The average sensor response for every odor is shown in Fig. 5. It can be observed that spoiled rice and rotten beef odors show high responses in the MQ-2 and MQ-7 sensors, which are typically sensitive to gases or strong volatile compounds. In contrast, spoiled milk and rotten pork odors produce high values in MQ-135 owing to decomposition byproducts such as ammonia and hydrogen sulfide. The temperature remained between 41.2 and 45.7 °C throughout the experiment, indicating controlled experimental conditions. The data from this graph demonstrate a clear distinction between different odor types and can be effectively applied in the development of E-nose systems or ML models for odor classification.

Figure 6 shows the average normalized confusion matrices for two classifiers, KNN and DT. The KNN and DT classifiers achieved high classification accuracies across all classes, with diagonal values ranging from 0.99 to 1.00. Most classes were predicted with nearly perfect accuracy. Both models made the same errors in Classes 2 (spoiled milk), 4 (rotten egg), and 6 (rotten pork), but DT made more errors in Class 0 (fungi).

4. Discussion

The experimental results showed that ML algorithms can effectively classify spoiled food odors using data collected from a portable E-nose. In terms of accuracy, among the six models evaluated, KNN outperformed all the others in terms of both accuracy and consistency, achieving the highest average classification accuracy of 99.889% with the lowest *SD* of 0.069514. This indicates that KNN is highly suitable for odor classification tasks using E-nose sensor data. While DT and SVM also produced high classification accuracies (99.843 and 99.504%, respectively), their performance was slightly less consistent than that of KNN.

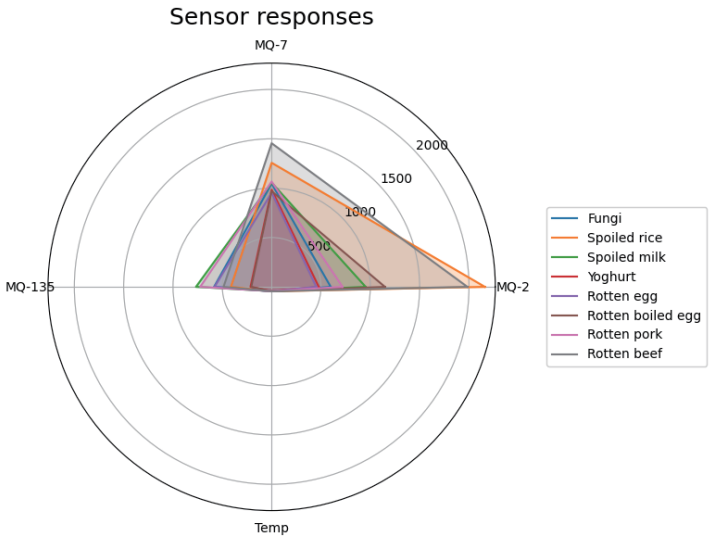

Fig. 5. (Color online) Radar plot of average sensor response value of every odor.

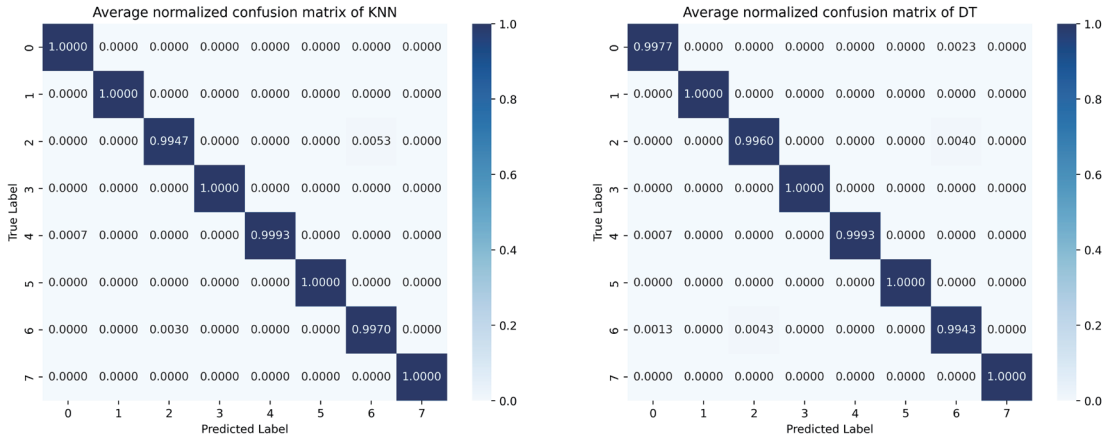

(a) (b)

Fig. 6. (Color online) Average normalized confusion matrix values of (a) KNN and (b) DT.

In terms of processing time, DT was indeed the most efficient, with an average processing time of 0.012080 s, making it highly desirable for applications demanding real-time responses. However, its average accuracy (99.843%) was slightly lower than that of KNN. KNN, while not the fastest, demonstrated an average processing time of 0.167477 s. Although DT is not the most accurate, this model offers a well-balanced trade-off for scenarios that prioritize rapid processing while the slight reduction in accuracy remains acceptable, making it suitable for real-time applications. This makes it highly recommended for real-time or near-real-time odor classification scenarios. NN takes longer to run than the other models because its structure is complex since it consists of multiple layers and a large number of weights that need to be updated through several iterations (epochs). Although the accuracy rate can be improved with additional training data, NN is not suitable for use in tools that require real-time responses, such as our E-nose, owing to the significant amount of time required for making predictions.

A separate validation set was not used in this study. After outlier removal with iForest, the dataset was reduced from 1800 to 1000 samples. To preserve enough training data, a 70/30 train–test split was applied, and each model was trained and tested ten times with results averaged to reduce random effects. As the goal was to demonstrate the feasibility of combining machine learning with a portable E-nose rather than fine-tuning hyperparameters, this approach was considered sufficient. Future work with larger datasets can include a validation or cross-validation set for more rigorous evaluation.

An important contribution of this study is that our proposed E-nose is significantly smaller and more compact than previous designs.[6,15,16] The RubiX WT1[16] E-nose contains more than ten sensors of different types, such as electrochemical (EC) gas sensors, MOS sensors, and photoionization detectors. It has a size of approximately 260 (height) × 160 (width) × 156.5 (depth) mm^3 , with a diameter of 99 mm, and weighs around 3 kg. In contrast, our device is significantly smaller and lighter, with dimensions of 205 × 160 mm^2 and a weight of approximately 150 grams. It includes low-cost sensors that offer fast response times, broad cross-sensitivity, and quick recovery, making it suitable for lightweight and responsive air quality monitoring applications.

These findings suggest that the integration of ML, particularly DT, with a well-designed portable E-nose can provide an efficient and accurate solution for odor classification. This system has potential applications in various fields, including food spoilage detection, environmental monitoring, and health diagnostics, where rapid and reliable odor detection is essential.

5. Conclusions

In this research, we focused on building a portable E-nose to detect spoiled food and provide alerts to the elderly, people with a reduced sense of smell, and the visually impaired, thus improving their quality of life. ML models were used, with odor data collected from an E-nose containing four sensors across eight odors. From the initial 1800 collected samples, preprocessing with iForest reduced the dataset to 1000 samples. We compared average accuracy and processing time over ten iterations. KNN achieved the highest average classification accuracy of 99.889%. Although KNN yields a higher accuracy, DT's average processing time is 0.012080 s, which is significantly faster than that of KNN by approximately 13.86 times, making it a good choice for accurate odor classification suitable for real-time portable E-nose devices. In future work, we aim to develop an E-nose system capable of sending alerts when it detects odors that are harmful to human health but barely detectable by the human nose. This includes the classification of odors that are mixed or masked by other scents, which presents a significant challenge. Addressing this issue will involve the application of advanced ML techniques capable of distinguishing and predicting complex odor mixtures based on sensor input data. Developing such capabilities will broaden the applicability of portable E-nose systems in real-world environments where odor signals are often ambiguous and overlapping.

Acknowledgments

Sincere appreciation is extended to S. Gongkam and T. Srathongkhao for their valuable contributions in identifying and acquiring the appropriate sensors used in this research.

References

1 Z. Zhai, Y. Liu, C. Li, D. Wang, and H. Wu: Sensors **24** (2024) 4806. https://doi.org/10.3390/s24154806
2 R. md, R. Yaacob, M. A Mohamed, T. M. Azahar, and F.A Rahim: Int. J. Eng. Technol. **7** (2018) 49. https://doi.org/10.14419/ijet.v7i3.28.20964
3 Y. Mao, L. Fang, X. Ye, S. Shi, Y. Qin, Z. Qin, Y. Cao, G. Jiang, and S. Tian: J. Food Compos. Anal. **140** (2025) 107302. https://doi.org/10.1016/j.jfca.2025.107302
4 P. Darvishi, E. Mirzaee-Ghaleh, Z. Ramedani, and H. Karami: Int. Dairy J. **157** (2024) 106012. https://doi.org/10.1016/j.idairyj.2024.106012
5 K. O. Kombo, N. Ihsan, T. S. Syahputra, S. N. Hidayat, M. Puspita, Wahyono, R. Roto, and K. Triyana: Sci. Afr. **24** (2024) e02153. https://doi.org/10.1016/j.sciaf.2024.e02153
6 A. Paleczek, and A. Rydosz: Sens. Actuators, B **408** (2024) 135550. https://doi.org/10.1016/j.snb.2024.135550
7 Y. Jiang, Z. Wang, Y. Hu, W. Lin, L. Yao, W. Xiao, J. Hu, W. Liu, C. Zheng, L. Chen, and X. Gao: Sens. Actuators, B **426** (2025) 136989. https://doi.org/10.1016/j.snb.2024.136989
8 D. Matatagui, F. A. Bahos, I. Gràcia, and M. d. C. Horrillo: Sensors **19** (2019) 5406. https://doi.org/10.3390/s19245406

9 G. Chen and G. Wu: J. Phys. Conf. Ser. **1894** (2021) 012080. https://doi.org/10.1088/1742-6596/1894/1/012080
10 J. Molina, L. F. Valdez, and J. M. Gutiérrez: Eng. Appl. Artif. Intell. **133** (2024) 108457. https://doi.org/10.1016/j.engappai.2024.108457
11 S. D. Astuti, I. R. Wicaksono, S. Soelistiono, P. A. D. Permatasari, A. K. Yaqubi, Y. Susilo, C. D. Putra, and A. Syahrom: Sens. Bio-Sens. Res. **43** (2024) 100632. https://doi.org/10.1016/j.sbsr.2024.100632
12 G. Domènech-Gil, and D. Puglisi: Sensors **22** (2022) 7340. https://doi.org/10.3390/s22197340
13 D. R. Wijaya, F. Afianti, A. Arifianto, D. Rahmawati, and V. S. Kodogiannis: Sens. Bio-Sens. Res. **36** (2022) 100495. https://doi.org/10.1016/j.sbsr.2022.100495
14 W. Ni, T. Wang, Y. Wu, X. Chen, W. Cai, and M. Zeng: IEEE Sens. J. **24** (2024) 671. https://doi.org/10.1109/JSEN.2023.3304355
15 C. Lu, M. Qing-Hao, L. A. J and Q. Pei-Feng: Meas. Sci. Technol. **32** (2021) 6. https://doi.org/10.1088/1361-6501/abef3b
16 J. Jońca, M. Pawnuk, A. Arsen, I. Sówka: Sensors **22** (2022) 1510. https://doi.org/10.3390/s22041510
17 Winsen Electronics: https://www.winsen-sensor.com/ (accessed January 2025).
18 F. T. Liu, K. M. Ting and Z. H. Zhou: Proc. 2008 Eighth IEEE Int. Conf. Data Mining (2008) 413− 422. https://doi.org/10.1109/ICDM.2008.17

About the Authors

Pikulkaew Tangtisanon received her B. Eng. and M. Eng. degrees in information technology engineering from King Mongkut's Institute of Technology Ladkrabang, Thailand, in 2003 and 2005, respectively, and her Ph.D. degree from Tokai University, Japan, in 2009. Since 2009, she has been a lecturer at King Mongkut's Institute of Technology Ladkrabang. Her research interests are in IoT, machine learning, and sensors. (pikulkaew.ta@kmitl.ac.th)

Boonyawee Grodniyomchai received his B.S. and M.S. degrees from King Mongkut's Institute of Technology Ladkrabang, Thailand, in 2016 and 2020, respectively. From 2024 to 2025, he was a teacher assistant at the School of Engineering, King Mongkut's Institute of Technology Ladkrabang, Thailand. Since 2020, he has been a Ph.D. student in electrical engineering at King Mongkut's Institute of Technology Ladkrabang. His research interests are in AI, machine learning, and electronic nose. (63601021@kmitl.ac.th)